Nuclear Physics **A469** (1987) 518–530
North-Holland, Amsterdam

TRANSVERSE ELECTROEXCITATION OF POSITIVE- AND NEGATIVE-PARITY STATES IN ^{19}F

A.J.H. DONNÉ[1]

Natuurkundig Laboratorium, Vrije Universiteit, P.O. Box 7161, 1081 HV Amsterdam, The Netherlands

L. LAPIKÁS

Nationaal Instituut voor Kernfysica en Hoge Energie Fysica, sectie K (NIKHEF-K), P.O. Box 4395, 1009 AJ Amsterdam, The Netherlands

A.G.M. VAN HEES and D. ZWARTS[2]

Rijksuniversiteit Utrecht, Fysisch Laboratorium, P.O. Box 80000, 3508 TA Utrecht, The Netherlands

Received 5 March 1987

Abstract: Transverse electroexcitation of states in ^{19}F at excitation energies below 4.4 MeV is described. Cross-section measurements were performed with the 500 MeV electron-scattering facility at NIKHEF-K at a scattering angle of 154° and in the momentum-transfer range $q = 1.4$–2.6 fm^{-1}. Some additional low-q data were measured with the 180° electron-scattering facility. The form factors for the negative-parity states are compared with predictions from a $1\hbar\omega$ shell-model calculation in the full 1p-2s1d configuration space. For the positive-parity states a comparison is made with $0\hbar\omega$ shell-model calculations in the full 2s1d configuration space and with $2\hbar\omega$ shell-model calculations in a space made up of all shells up to the $1f_{7/2}$ orbit. The large differences observed between the form factors calculated in the $0\hbar\omega$ and $2\hbar\omega$ spaces are ascribed to effects of space truncation.

E NUCLEAR REACTIONS ^{19}F(e, e'), $E = 46$–272 MeV; measured $\sigma(E, \theta)$, ^{19}F deduced transverse form factors. Shell-model calculation.

1. Introduction

Many aspects of ^{19}F make this nucleus particularly interesting for the investigation of nuclear structure phenomena. Its study has stimulated progress in our understanding of the nuclear shell model ever since the pioneering work of Elliott *et al.* [1]) and Redlich [2]). Previous electron-scattering experiments [3-8]), as well as measurements of electromagnetic transition strengths [9-13]), indicate that the ground state and low-lying excited states of ^{19}F can be viewed as belonging to rotational bands of a strongly deformed nucleus. The facts that ^{19}F corresponds in the simple shell model to a system of only three active nucleons outside the ^{16}O core and that it is strongly deformed, make it an excellent laboratory to study core-polarization effects.

[1] Present address: FOM-Instituut voor Plasmafysica, P.O. Box 1207, 3430 BE Nieuwegein, The Netherlands.

[2] Present address: KSEPL, P.O. Box 60, 2280 AB Rijswijk, The Netherlands.

Several types of theoretical calculations have been performed to describe the properties of ^{19}F. Among them are various shell-model calculations which differ from each other by the size of the employed configuration space, the mass dependence of the parameters and the way in which the two-body matrix elements have been determined [7,8,14-16]).

Recently, measurements of elastic magnetic electron scattering from ^{19}F have been reported [7,8]). Shell-model calculations in the complete 2s1d configuration space were not able to account for the presence of the second maximum at 1.3 fm^{-1} in the experimental form factor. From a large-basis shell-model calculation in the (1s)-(1p)-(2s1d)-(1f$_{7/2}$) configuration space, restricted to $0\hbar\omega$ and $2\hbar\omega$ excitations, it became clear that small admixtures of $2\hbar\omega$ components, which make up only a few percent of the ground-state wave function, cause considerable changes in the elastic magnetic form factor of ^{19}F. Although no quantitative agreement was obtained with the experimental data, the calculated form factor exhibited the correct shape. First-order core-polarization theory starting from a shell-model calculation using the full 2s1d configuration space, gave similar results. In spite of these successes we note that the necessity for including $2\hbar\omega$ excitations for the description of the elastic magnetic form factor does not follow unambiguously from the data. As described in ref. [8]) a satisfactory description within the 2s1d configuration space is possible, if the amplitudes of the three contributing 2s1d matrix elements are treated as free parameters. A similar conclusion was reached recently by Bouten and Bouten [17]), who showed that within the framework of a projected Hartree-Fock (PHF) calculation "simple" 2s1d wave functions can be found that describe the data just as well as deformed PHF wave functions. Hence we conclude that more experimental data than the elastic magnetic form factor alone are needed to study the importance of $2\hbar\omega$ excitations.

In the forelying paper we compare the predictions of the present large-basis shell-model calculation for ^{19}F, which is the first one not being based on an inert core, with inelastic electron-scattering data. For this purpose transverse form factors are especially suitable, since they are much more sensitive to $2\hbar\omega$ excitations than longitudinal form factors. We therefore carried out the electron-scattering experiment described below at backward angles only.

Inelastic electron-scattering form factors of ^{19}F have earlier been measured at Bates [7]) in the momentum-transfer range $q = 0.8$–2.4 fm^{-1} at scattering angles of 45°, 90°, and 160°. However, the transverse form factors were only determined with limited accuracy. In this paper, we present transverse electron-scattering form factors for all known states of ^{19}F up to an excitation energy of 4.4 MeV [ref. [18])]. The data include the major part of the levels belonging to the rotational bands built upon both the $K^\pi = \frac{1}{2}^+$ ground state and the $K^\pi = \frac{1}{2}^-$ first-excited state. The data were mainly obtained in the momentum-transfer range $q = 1.4$–2.6 fm^{-1} with the 500 MeV (154°) electron-scattering facility at NIKHEF-K [19]). Some low-energy data were measured with the 180° scattering facility at NIKHEF-K [20]).

The main emphasis of this paper is on the comparison of the present experimental data with predictions from recent shell-model calculations [7,8]). Since the experimental procedure and the shell-model calculations have been described extensively elsewhere [7,8]), only some supplementary considerations are given in sect. 2 and sect. 3, respectively. The experimental results, presented in sect. 4, are discussed in the context of shell-model theories. Conclusions are summarized in sect. 5.

2. Experiment

Since all data for inelastic scattering from ^{19}F presented in this paper have been collected in the same experimental runs as those for the ground state, we refer to ref. [8]) for details on the experimental arrangement and data acquisition. Most of the inelastic data were taken in the momentum-transfer range $q = 1.4$–$2.6\ \mathrm{fm}^{-1}$ in the 500 MeV station [19]) with the QDD spectrometer at a scattering angle of 154°. The measurements were carried out with Teflon $(CF_2)_n$ and polyvinylidenefluoride $(CH_2CF_2)_n$ targets (30 mg/cm^2), which were used in reflection geometry and mounted in a rotating device to spread heat dissipation. Nevertheless, it appeared during test runs that the abundancy of ^{19}F and ^{12}C atoms in these targets changed as a function of irradiation dose. These effects were taken care of by dividing each measurement into short runs corresponding to a collected charge of 10 to 50 μC. For each run the amounts of ^{19}F and ^{12}C were determined from the contents of a couple of well-isolated strong ^{19}F and ^{12}C peaks in the spectra; these were subsequently used for normalization [see ref. [21])].

The spectra were corrected for kinematic broadening (for $A = 19$), spectrometer optical aberrations, dead-time losses and wire inefficiencies. The primary beam energy was obtained through an internal calibration procedure that makes use of several strong ^{19}F peaks of well-known excitation energies. Due to the good overall resolution ($\Delta p/p < 10^{-4}$) virtually all final states could be resolved.

Only for the $\frac{5}{2}^+$ level at 197 keV and the $\frac{9}{2}^+$ level at 2.78 MeV information was also obtained at low incident beam energies with the 180° scattering facility [19]). These measurements have been described elsewhere [8]).

Inelastic electron scattering from ^{19}F has been extensively studied at Bates [7]) in the momentum-transfer range $q = 0.8$–$2.4\ \mathrm{fm}^{-1}$ at scattering angles of 45°, 90° and 160°. In this experiment, the longitudinal contributions to the form factors were determined more accurately than the transverse contributions. Since the present experimental cross sections σ_{exp} were measured at backward scattering angles only, the longitudinal form factors could not be determined. In order to correct the present data for longitudinal contributions Fourier-Bessel (FB) fits [22]) were made to the longitudinal data from Bates [7]). The transverse cross sections σ_{T} were then obtained from

$$\sigma_{\mathrm{T}} = \sigma_{\mathrm{exp}} - \sigma_{\mathrm{L}}(154°)\,,$$

where $\sigma_L(154°)$ is the longitudinal cross section calculated with the fitted FB coefficients. The quality of the FB fits for the levels of interest was satisfactory (χ^2/d.f. < 2) in all cases. Finally we determined experimental transverse form factors $F_T(q)$ through

$$F_T^2 = \sigma_T / \sigma_{Mott}(1/2 + \tan^2 \tfrac{1}{2}\theta) ,$$

where σ_{Mott} is the Mott cross section including recoil but without the factor Z.

3. Theory

Extensive shell-model calculations for states in ^{19}F up to $E_x = 8$ MeV have been performed by Brown *et al.* [7]). The transitions to the positive-parity states (including the ground state) were calculated in the full 2s1d ($0\hbar\omega$) configuration space. The hamiltonian used in these calculations was a mass-dependent 2s1d-shell interaction which was fitted to energy levels of a large number of 2s1d-shell nuclei. For the transition to the negative-parity states, the 1p-2s1d ($1\hbar\omega$) configuration space was used with the particle-hole interaction of Millener and Kurath. This hamiltonian was chosen to account for the non-normal parity states in a number of nuclei ranging from ^{11}Be to ^{16}O. For the particle-particle sd-shell interaction in these calculations, the one of Preedom and Wildenthal was used, and for the p-shell hole-hole interaction the one of Cohen and Kurath. The radial wave functions required for the single-nucleon transition densities were taken to be harmonic-oscillator states. The oscillator length parameter $b = 1.833$ fm was chosen to reproduce the rms charge radius of 2.898 ± 0.010 fm for ^{19}F obtained from muonic-atom data [23]). In both the $0\hbar\omega$ and the $1\hbar\omega$ models, free-nucleon orbital and spin g-factors and free-nucleon charges were used to calculate the transverse form factors.

For the analysis of the present data we performed large-basis shell-model calculations for the positive-parity states in a truncated $2\hbar\omega$ space by including only the components with seniority less than five, while specifying that all single-particle states beyond the $1f_{7/2}$ orbit are unoccupied [8]). This truncation might cause spurious admixtures which are, however, expected to be negligible for positive-parity states [24]). In the effective interaction we used low-order Talmi integrals [24]), which were empirically determined in order to reproduce the binding energy and the experimental spectrum of the positive-parity states of ^{19}F. The higher-order Talmi integrals, which describe the long-range behaviour of the effective interaction, were computed with the realistic Reid soft-core potential [25]). Since the applied truncation of the model space is rather arbitrary and the renormalization of the interaction is based on the experimental data of only one nucleus, the calculations have to be considered as a first investigation of the effects of a larger model space, more than as the final result.

In the $2\hbar\omega$ calculation we used free-nucleon g-factors and charges. For the radial size of the harmonic oscillator potential we chose $b = 1.77$ fm, consistent with the oscillator quantum $\hbar\omega = 13.2$ MeV used explicitly in this shell-model calculation.

The computation of transitions to the negative-parity states with the large-basis model would require a (truncated) $3\hbar\omega$ configuration space. This is still beyond the capability of present-day vector-processing supercomputers.

4. Results

We first present the results for electroexcitation of the positive-parity states belonging to the ground-state rotational band. The second $\frac{3}{2}^+$ level at 3.908 MeV, which is no member of this band, will be discussed separately. The results of the $0\hbar\omega$ calculations by Brown *et al.*[7]) and of the present $2\hbar\omega$ calculations will be compared to the experimentally determined form factors. The data for the negative-parity levels of ^{19}F will be presented along with results from the $1\hbar\omega$ calculation by Brown *et al.*[7]). The three shell-model calculations will be referred to as $0\hbar\omega$, $1\hbar\omega$, and $2\hbar\omega$ model, respectively.

All form factors were calculated in plane-wave Born approximation. Coulomb-distortion effects were corrected for by transforming the experimental q-values to effective momentum-transfer values through

$$q_{\text{eff}} = q(1 + f_c Z\alpha\hbar c / E_i R) ,$$

where R is the equivalent radius of the charge distribution, defined by $R^2 = \frac{5}{3}\langle r^2\rangle$. From a comparison of PWBA and DWBA calculations for different multipolarities, we determined the factor f_c to be 0.95, close to that for the ground state[8]).

In the figures presented below we only plotted the data of the present experiment for reasons of clarity. The consistency between our data and those of Brown *et al.*[7]) is shown for some ^{19}F levels in ref.[8]).

4.1. THE $K^\pi = \frac{1}{2}^+$ ROTATIONAL BAND

The transverse form factors for the ^{19}F levels belonging to the ground-state rotational band and at excitation energies below 4.4 MeV are presented in figs. 1–4. In these figures the calculated contributions from electric and magnetic multipoles to the form factor are shown separately. The results of the $0\hbar\omega$ model are plotted in figs. 1a–4a, whereas those of the $2\hbar\omega$ model are shown in figs. 1b–4b.

The electric quadrupole form factor for the $\frac{5}{2}^+$ state at 197 keV as calculated with the $2\hbar\omega$ model (see fig. 2b) is the only form factor with a non-negligible, albeit small, contribution from outside the 2s1d-shell. All other form factors calculated with the $2\hbar\omega$ model contain only significant contributions from the 2s1d-shell matrix elements. Therefore, any difference between the results of the $0\hbar\omega$ and the $2\hbar\omega$ model must be attributed to a renormalization of the 2s1d-shell matrix elements due to the larger configuration space used in the $2\hbar\omega$ calculation.

For the $\frac{3}{2}^+$ state at 1.55 MeV (see fig. 1) the amplitude of the first maximum is predicted better by the $2\hbar\omega$ model, but both models predict the amplitude of the

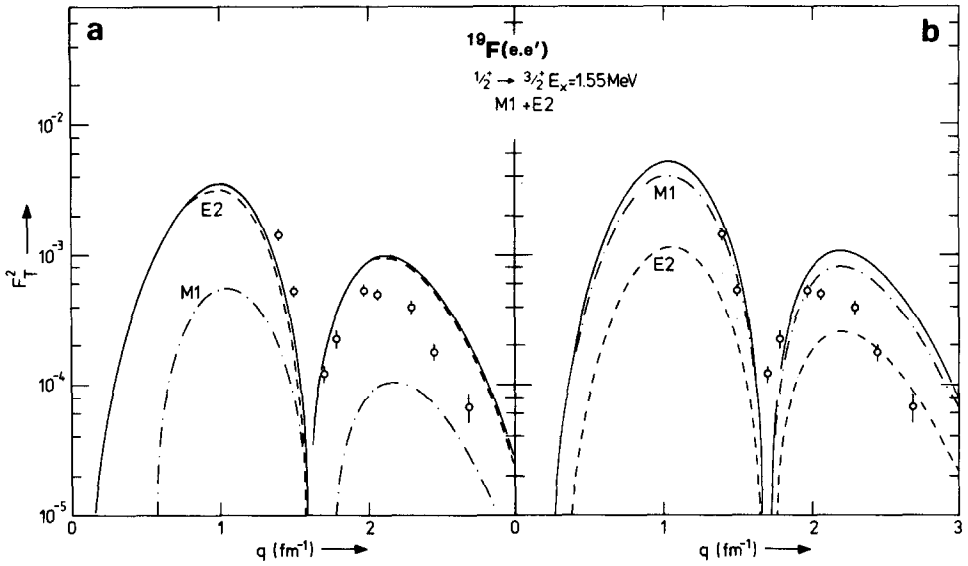

Fig. 1. Experimental and theoretical transverse form factors for the $\frac{3}{2}^+$ level at 1.55 MeV. The result of the $0\hbar\omega$ calculation is shown in fig. 1a, that of the $2\hbar\omega$ calculation in fig. 1b. The dashed curves represent the electric contributions, whereas the dot-dashed curves represent the magnetic contributions to the total form factor (solid curves). The open circles represent data measured at 154°.

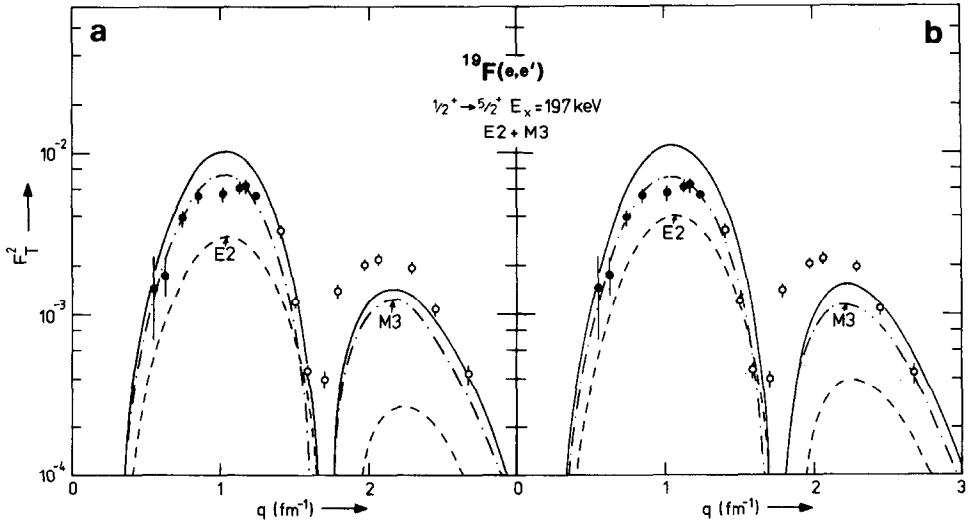

Fig. 2. Same as fig. 1, but for the $\frac{5}{2}^+$ level at 197 keV. The black circles represent data measured at 180°.

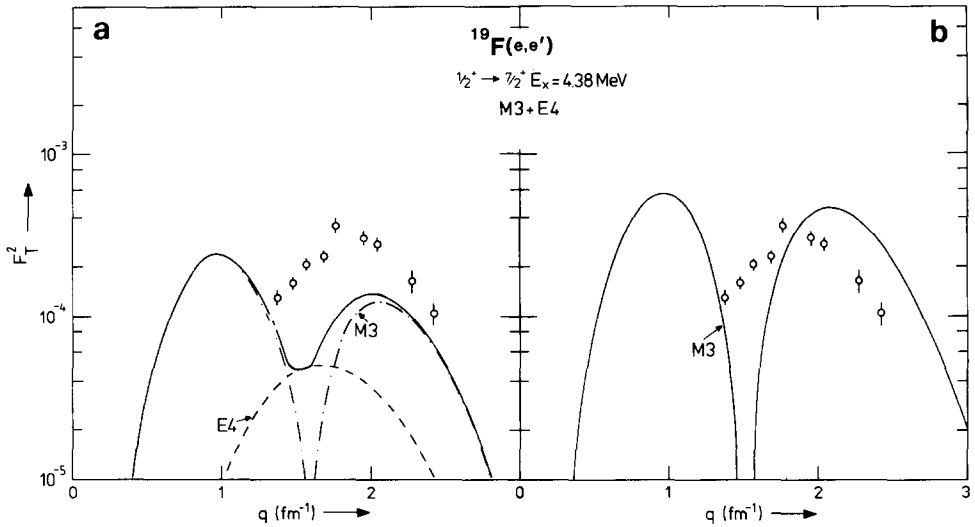

Fig. 3. Same as fig. 1, but for the $\frac{7}{2}^+$ level at 4.38 MeV.

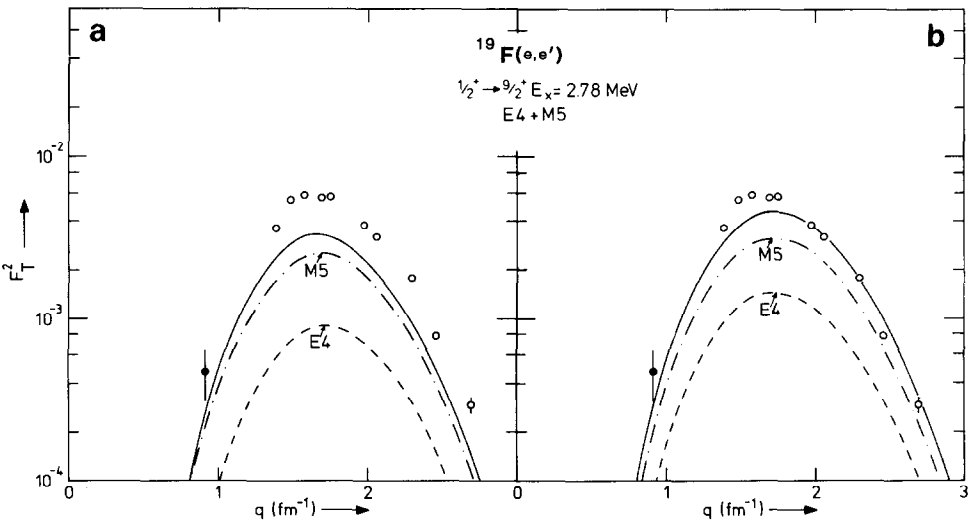

Fig. 4. Same as fig. 1, but for the $\frac{9}{2}^+$ level at 2.78 MeV. The black circle represents a data point measured at 180°.

second maximum about a factor of 2 too high. Note that the E2 form factor is the most important contribution to the total form factor in the $0\hbar\omega$ calculation, whereas in the $2\hbar\omega$ model the M1 form factor is the dominating one.

For the $\frac{5}{2}^+$ level at 197 keV data were taken also at 180°. The results of the two shell-model calculations for this state are nearly equal (see fig. 2), despite a non-negligible contribution from the $1s_{1/2}$-$1d_{5/2}$ transition in the E2 form factor calculated

with the $2\hbar\omega$ model. Both models predict the wrong amplitudes for the first and second maximum in the form factors.

None of the models can describe the experimental data for the $\frac{7}{2}^+$ level at 4.38 MeV (see fig. 3). In this case a mixture of M3 and E4 contributions that is totally different from theory is needed to explain the data. We also note that Brown *et al.* [7]) have demonstrated that it is doubtful whether this $\frac{7}{2}^+$ state may be identified as a member of the ground-state rotational band.

The low-energy data point for the $\frac{9}{2}^+$ level at 2.78 MeV was measured at 180°. Both models give similar predictions for the form factor of this state, which is not surprising since there are only few single-particle transitions which can contribute to it. The amplitude and the high-q behaviour of the form factor as calculated with the $2\hbar\omega$ model is in better agreement with experiment than those calculated with the $0\hbar\omega$ model.

4.2. THE $\frac{3}{2}^+$ LEVEL AT 3.91 MeV

For the $\frac{3}{2}^+$ level at 3.91 MeV there are enormous differences between the $0\hbar\omega$ model (see fig. 5a) and the $2\hbar\omega$ model (see fig. 5b). In the $0\hbar\omega$ model the predictions for the $\frac{3}{2}^+$ levels at 1.55 MeV (see fig. 1a) and at 3.91 MeV are very similar. The reason for this is that the main configuration for the first $\frac{3}{2}^+$ state is found to be

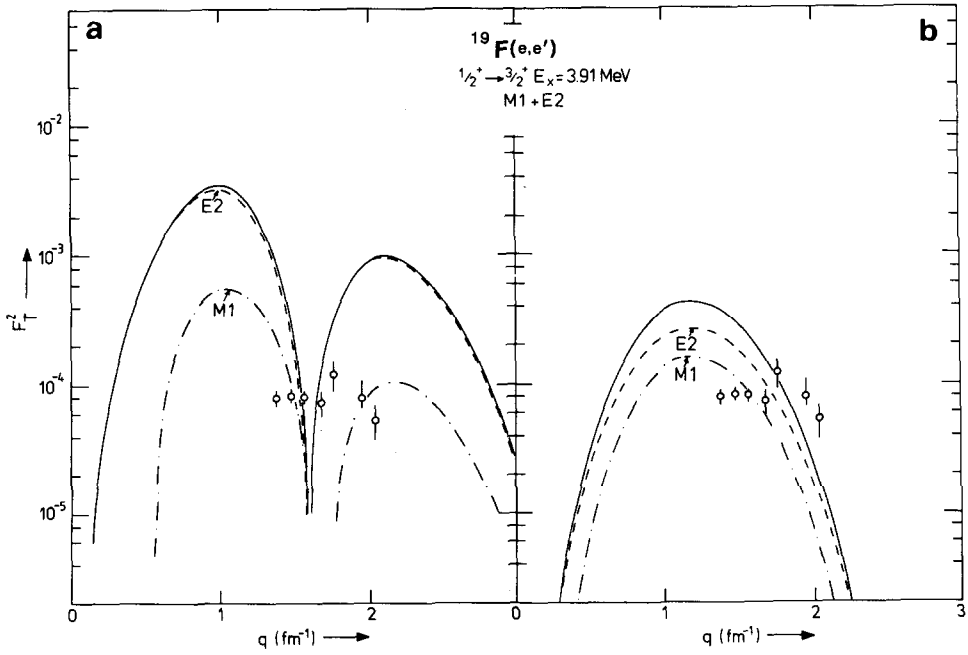

Fig. 5. Same as fig. 1, but for the $\frac{3}{2}^+$ level at 3.91 MeV.

$\pi(1d_{3/2})_{3/2,1/2}\nu(1d_{5/2})^2_{0,1}$, whereas for the second $\frac{3}{2}^+$ state it is $\pi(1d_{3/2})_{3/2,1/2}\nu(2s_{1/2})^2_{0,1}$. The $2\hbar\omega$ model is in better quantitative agreement with the data; the shape of the form factor, however, is incorrect. Although there are small contributions from outside the 2s1d shell in the $2\hbar\omega$ calculation, the most important reason for the difference between the two models is again a strong renormalization of the 2s1d matrix elements in the larger configuration space.

4.3. THE $K^\pi = \frac{1}{2}^-$ ROTATIONAL BAND

The transverse form factors for the ^{19}F levels belonging to the $K^\pi = \frac{1}{2}^-$ rotational band and at excitation energies below 4.4 MeV are presented in fig. 6. In this figure contributions from magnetic and electric multipoles to the form factors calculated with the $1\hbar\omega$ model are shown separately.

Excitation of the $\frac{1}{2}^-$ level at 110 keV proceeds by a pure E1 transition. The shape of the form factor is reproduced well; the calculated strength, however, is a factor of 1.4 smaller than the experimental value. At momentum transfers below $q = 1.2$ fm^{-1} the size of the form factor is overestimated by the theory. Although this is not obvious from fig. 6, this can be concluded from the present measurements on the - unresolved - lowest-lying three levels of ^{19}F. If the theoretical shape of the E1 form factor at low q is assumed to be correct, the strength of the $\frac{1}{2}^-$ excitation for $q < 1.2$ fm^{-1} would be larger than the total strength of the three lowest-lying levels [8]. This would imply that the ground state and the $\frac{5}{2}^+$ state have negligible strength, which is in contradiction with other experiments [5-7]. Furthermore, a Fourier-Bessel fit to the E1 form factor of the $\frac{1}{2}^-$ state gives a much steeper fall-off of the form factor below $q = 1$ fm^{-1} [see ref. [8]]. This indicates that the radial extension of the involved wave functions is possibly too large. A 5 to 10% decrease in the employed oscillator parameter would be needed to adapt the low-q behaviour and to bring the curve into agreement with the data at high q.

The shape of the theoretical form factor for the $\frac{3}{2}^-$ level at 1.46 MeV is consistent with the present data (see fig. 6). The data point at $q = 2.05$ fm^{-1} indicates, however, that an additional form factor maximum at high q may be present. Such a maximum does appear in the M2 contribution to the theoretical form factor, but it is too small to reproduce the experimental data. On the other hand we note that below $q = 2$ fm^{-1} the M2 form factor is overestimated by a factor of 1.5.

For the $\frac{5}{2}^-$ state at 1.35 MeV the shape of the theoretical form factor is also close to the experimental shape (see fig. 6). The maximum is, however, predicted at too large a momentum transfer and the theory is enhanced with respect to experiment.

It was not possible to separate the $\frac{7}{2}^-$ level at 4.00 MeV and the $\frac{9}{2}^-$ level at 4.03 MeV at the highest five q-values in the present experiment. The available low-q data for the $\frac{7}{2}^-$ level are slightly overestimated by the theoretical form factor (see fig. 6). At the higher q-values the transverse form factor for the $\frac{9}{2}^-$ state was deduced by subtracting an extrapolated transverse form factor for the $\frac{7}{2}^-$ state and the longitudinal

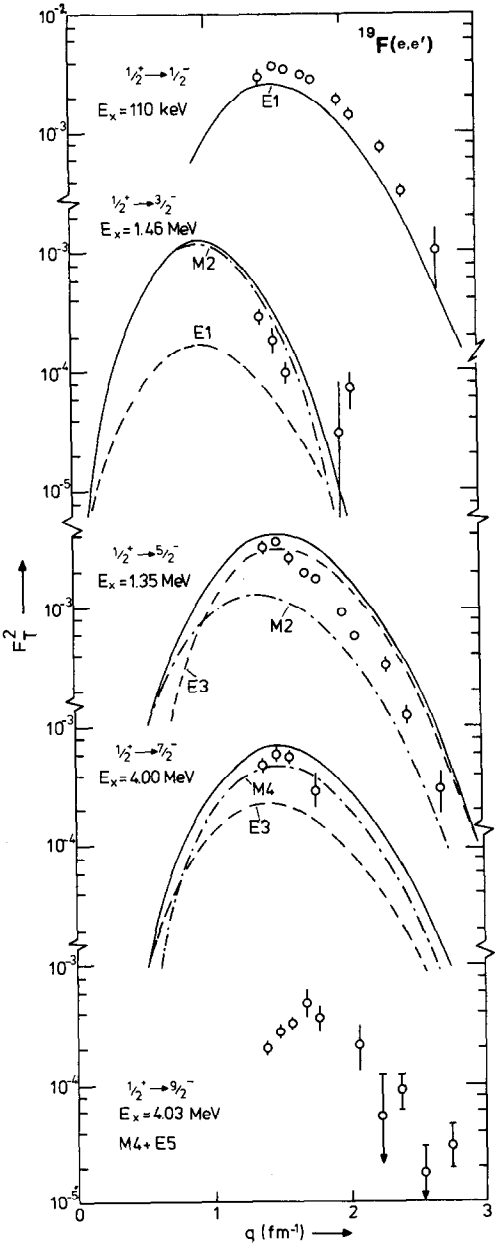

Fig. 6. Experimental and theoretical form factors for the negative-parity states belonging to the $K^\pi = \frac{1}{2}^-$ rotational band. Experimental data measured at 154° are indicated by the open circles. The magnetic (dot-dashed) and electric (dashed) contributions to the total form factor (solid curve) calculated with the $1\hbar\omega$ model have been indicated.

form factors for both states from the total experimental form factor for this unresolved doublet. For the extrapolation of the $\frac{7}{2}^-$ contribution to higher q we used the shape of the $1\hbar\omega$ form factor for this state (see fig. 6), scaled to fit our transverse low-q data. As a consequence of this model-dependent procedure the experimental data for the $\frac{9}{2}^-$ level have large error bars. Nevertheless, one observes a form-factor maximum around $q = 2\,\mathrm{fm}^{-1}$, which strongly suggests an E5 component in this transition. However, within the 1p-2s1d configuration space such a component is forbidden, whereas the calculated [7]) M4 component is two orders of magnitude smaller and has a maximum at about $q = 1.5\,\mathrm{fm}^{-1}$.

5. Conclusions

We have presented experimental data for transverse inelastic electron scattering to positive- and negative-parity states in ^{19}F up to an excitation energy of 4.4 MeV. The data have been compared with existing shell-model calculations [7]) in a $0\hbar\omega$ and $1\hbar\omega$ configuration space. In order to study the effects of space truncation we calculated the form factors also in an extended $2\hbar\omega$ space.

For the *negative*-parity states we observe that the shape of the form factors predicted from $1\hbar\omega$ shell-model calculations [7]) in the 1p-2s1d configuration space is in reasonable agreement with experiment. However, in most cases the predicted form factors overshoot the experimental values by 25 to 50%. This corresponds to a quenching of the data that is similar to the one observed [26]) for particle-hole transitions to stretched states for a large range of nuclei. Hence an explanation in terms of a partial occupancy of valence states might be considered. Also it would be interesting to study how a $3\hbar\omega$ calculation would alter the renormalization of the matrix elements for the non-natural parity transitions. Such an effect might already be expected from the difference between the calculated $0\hbar\omega$ and $2\hbar\omega$ form factors. Moreover, the extension to a $3\hbar\omega$ space is needed to explain the relatively large E5 component of the transition to the $\frac{9}{2}^-$ state at 4.03 MeV.

For the *positive*-parity states we can find no conclusive evidence for the need of $2\hbar\omega$ admixtures. Both the $0\hbar\omega$ and the $2\hbar\omega$ models give a reasonable prediction for some levels, but their calculated form factors deviate severely from experiment for other states. From the comparison of the two models with experiment it is impossible to conclude which of them gives the better predictions for ^{19}F. The inclusion of q-independent effective charges in the electric contributions to the form factors would not alter this observation.

The observed discrepancy between measured and calculated form factors of ^{19}F requires further theoretical study. Since the (e, e′) process is described by a one-body operator, one-particle one-hole (1p-1h) excitations might play an important role. In the $0\hbar\omega$ calculations none of these excitations are included. In the present $2\hbar\omega$ calculations the 1p-1h contributions $1s \rightarrow 2s$ have been taken into account only, whereas, because of computational limitations the contributions from higher orbits

have been restricted to the lowest-lying 1f2p orbit, i.e. the $(1f_{7/2})^2$ configurations. Hence, it would be interesting to investigate whether or not a better understanding of the present data can be obtained by the inclusion of effects of $1p \rightarrow 2p$ as well as $2s1d \rightarrow 3s2d$ transitions in the $2\hbar\omega$ space. These transitions may be expected to change the shape of the form factors considerably since wave functions with a different number of radial nodes are involved. In order to make such calculations feasible, one may have to exclude 2p-2h excitations. This is justified because the latter excitations do not contribute directly to the (e, e′) cross sections.

We would like to thank Drs. G. van Middelkoop, P.W.M. Glaudemans and A.E.L. Dieperink for stimulating discussions and a critical reading of the manuscript. This work is part of the research programme of the National Institute for Nuclear Physics and High Energy Physics (NIKHEF) and the Free University (VU), made possible by financial support from the Foundation of Fundamental Research on Matter (FOM) and the Netherlands' Organisation for the Advancement of Pure Scientific Research (ZWO).

References

1) J.P. Elliott and B.H. Flowers, Proc. R. Soc. London, **A229** (1955) 536
2) M.G. Redlich, Phys. Rev. **99** (1955) 1427
3) T. Walcher and P. Strehl, Z. Phys. **232** (1970) 342
4) P.L. Hallowell, W. Bertozzi, J. Heisenberg, S. Kowalski, X. Maruyama, C.P. Sargent, W. Turchinetz, C.F. Williamson, S.P. Fivozinsky, J.W. Lightbody and S. Penner, Phys. Rev. **C7** (1973) 1396
5) M. Oyamada, T. Terasawa, K. Nakahara, Y. Endo, H. Saito and E. Tanaka, Phys. Rev. **C11** (1975) 1578
6) C.F. Williamson, F.N. Rad, S. Kowalski, J. Heisenberg, H. Crannell, J.T. O'Brien and H.C. Lee, Phys. Rev. Lett. **40** (1978) 1702
7) B.A. Brown, B.H. Wildenthal, C.F. Williamson, F.N. Rad, S. Kowalski, H. Crannell and J.T. O'Brien, Phys. Rev. **C32** (1985) 1127
8) A.J.H. Donné, G. van Middelkoop, L. Lapikás, T. Suzuki, P.W.M. Glaudemans and D. Zwarts, Nucl. Phys. **A455** (1986) 453
9) P.H. Stelson and F.K. McGowen, Nucl. Phys. **16** (1960) 92
10) A.E. Litherland, M.A. Clark and C. Broude, Phys. Lett. **3** (1963) 204
11) J.A. Becker, J.W. Olness and D.H. Wilkinson, Phys. Rev. **155** (1967) 1089
12) T.K. Alexander, O. Hausser, K.W. Allen and A.E. Litherland, Can. J. Phys. **47** (1969) 2335
13) A.R. Poletti, J.A. Becker and R.E. McDonald, Phys. Rev. **182** (1969) 1054
14) T. Inoue, T. Sebe, H. Hagiwara and A. Arima, Nucl. Phys. **59** (1964) 1
15) B.A. Brown, R. Radhi and B.H. Wildenthal, Phys. Lett. **113B** (1983) 5
16) J. van Hienen, private communication
17) M. Bouten and M.C. Bouten, Nucl. Phys. **A459** (1986) 253
18) F. Ajzenberg-Selove, Nucl. Phys. **A392** (1983) 1
19) C. de Vries, C.W. de Jager, L. Lapikás, G. Luijckx, R. Maas, H. de Vries and P.K.A. de Witt Huberts, Nucl. Instr. Meth. **223** (1984) 1
20) A.J.H. Donné, G. van Middelkoop, L. de Vries, L. Lapikás, J.B. van der Laan, C. de Vries and J.G. Noomen, Nucl. Instr. Meth. **224** (1984) 97
21) A.J.H. Donné, Ph.D. thesis, Vrije Universiteit, Amsterdam, 1985, The Netherlands
22) J. Heisenberg, Adv. in Nucl. Phys. **12** (1981) 61

23) L.A. Schaller, T. Dubler, K. Kaesser, G.A. Rinkler, B. Robert-Tissat, L. Schellenberg and H. Schneuwly, Nucl. Phys. **A300** (1978) 225
24) D. Zwarts, Ph.D. thesis, Rijksuniversiteit Utrecht, 1984, The Netherlands
25) R. Reid, Ann. of Phys. **50** (1968) 41
26) C.N. Papanicolas, Proc. Workshop on nuclear structure at high spin, excitation, and momentum transfer, Bloomington, 1985